THE ASTROPHYSICAL JOURNAL, 376:608–614, 1991 August 1

1991ApJ...376..608G

NGC 7538 IRS 1: SUBARCSECOND RESOLUTION RECOMBINATION LINE AND $^{15}NH_3$ MASER OBSERVATIONS

R. A. GAUME, K. J. JOHNSTON, AND H. A. NGUYEN
Center for Advanced Space Sensing, Code 4213.6, Naval Research Laboratory, Washington, DC 20375-5000
T. L. WILSON
Max-Planck-Institut für Radioastronomie, Auf dem Hügel 69, 53 Bonn, 1, Germany
H. R. DICKEL
Astronomy Department, 1002 West Green Street, University of Illinois, Urbana, IL 61801
W. M. GOSS
National Radio Astronomy Observatory, P.O. Box 0, Socorro, NM 87801
AND
M. C. H. WRIGHT
Radio Astronomy Laboratory, University of California, Berkeley, CA 94720
Received 1990 September 14; accepted 1991 January 30

ABSTRACT

The $^{15}NH_3$ $(J, K) = (3, 3)$ maser emission associated with NGC 7538 IRS 1 has been imaged with 0".2 resolution. The masers are distributed in a 0".2 region coincident with the 1.3 cm wavelength continuum core of the NGC 7538 IRS 1 H II region. The strongest $^{15}NH_3$ masers are found concentrated in two regions separated by approximately 0".2. These masers may be amplifying the strong double-lobe radio continuum core of the IRS 1 H II region. The velocities of the $^{15}NH_3$ masers range from -62 to -53 km s^{-1} and show a systematic velocity gradient from SW (-62 km s^{-1}) to NE (-52 to -54 km s^{-1}). The orientation of this gradient is similar to that found by Scoville et al. (1986) for the ^{13}CO emission toward IRS 1. Observations of several hydrogen recombination line transitions are reported. These observations show that the velocity of the IRS 2 H II region is similar to that of the ambient molecular cloud, ≈ -65 km s^{-1}. However, unlike IRS 2, the IRS 1 H II region is significantly redshifted with respect to the molecular cloud. The velocity of the IRS 1 H II region, as determined from H 76α data, is ≈ -22 km s^{-1}. We interpret this as implying that the ionized gas is champagne flowing off the foreground molecular cloud.

Subject headings: infrared: sources — interstellar: molecules — masers — nebulae: H II regions — nebulae: individual (NGC 7538)

1. INTRODUCTION

Stars form from molecular clouds, and once formed, may interact with these clouds, perhaps to produce a new generation of stars. In fact, observational evidence has emerged that the star-formation process quite often includes one or several periods in which newly formed stars interact with their parent molecular cloud. The most common examples are bipolar outflows seen in CO (see e.g., Lada 1985). However, other tracers probe these interactions on differing scale lengths, and under differing physical conditions. In particular, molecular maser line emission is associated with ongoing massive star formation (see, e.g., Reid & Moran 1981). These maser line emitting regions have large H_2 densities and small internal velocity motions. These two characteristics indicate that such regions are excellent places to search for protostar candidates.

NGC 7538 is one of the most studied regions of star formation in the Galaxy. Located in Perseus, at a distance of approximately 3 kpc, the NGC 7538 complex has been the object of numerous optical, infrared, and radio observations. The complex consists of an optically visible H II region and at least three compact infrared components, IRS 1–3. The component IRS 1, also known as NGC 7538 B (Martin 1973), is an ultracompact H II region in the radio continuum. The component IRS 1 has an angular extent of several arcseconds at centimeter wavelengths and is extended in the N-S direction. With subarcsecond resolutions, IRS 1 has been shown to consist of several emission "hotspots" (see e.g., Campbell 1984). The core of IRS 1 has been resolved into two individual radio lobes separated by 0".2 (Turner & Matthews 1984; Campbell 1984). Pratap, Batrla, & Snyder (1989) have discussed evidence for a mass outflow from IRS 1. In this model, the two radio lobes may be the two halves of a collimated outflow from a central massive star. Scoville et al. (1986) have mapped a ^{12}CO outflow near IRS 1 which is directed NW-SE; they also find a rotating ^{13}CO structure, centered on IRS 1. The rotating ^{13}CO structure has recently been confirmed by Pratap, Snyder, & Batrla (1991). The molecular gas traced by the rotating ^{13}CO structure may help constrain the expansion of the H II region. Shock-excited emission from vibrationally excited levels of molecular hydrogen (Fischer et al. 1980) has also been detected.

Near NGC 7538 IRS 1 is the largest collection of masers from different molecular species found so far. Maser line emission has been found for OH (see, e.g., Dickel et al. 1982), H_2O (see, e.g., Kameya et al. 1990), methanol (Menten et al. 1986), formaldehyde (Rots et al. 1981), NH_3 (Madden et al. 1986), and $^{15}NH_3$ (Johnston et al. 1989). The $^{15}NH_3$ observations of Johnston et al. (1989) found these masers to be coincident with the core continuum peak of IRS 1, distributed across a region extended approximately 0".4 in the north-south direction; there was also evidence for a velocity gradient from north to south.

However, the 1".2 resolution of the Johnston et al. (1989) data prevented a detailed examination of the kinematics of the $^{15}NH_3$ masers. This paper extends the work of Johnston et al. (1989) by imaging the $^{15}NH_3$ masers found toward NGC 7538 IRS 1 with observations employing higher spatial and spectral resolution, and covering a larger total velocity range. In addition to the $^{15}NH_3$ observations reported in this paper, hydrogen recombination line observations of the IRS 1 and IRS 2 H II regions are also presented.

2. OBSERVATIONS AND RESULTS

2.1. $^{15}NH_3$

The $(J, K) = (3, 3)$ transition of $^{15}NH_3$ toward NGC 7538 IRS 1 was observed using all 27 antennas of the Very Large Array (VLA) of the National Radio Astronomy Observatory[1] on 1989 March 12. The VLA was in the B-configuration, which provides baselines ranging in length from 0.21 to 11.4 km. The total integration time on NGC 7538 was 6 hr. One hundred twenty-eight spectral channels across a bandwidth of 3.125 MHz provided a velocity resolution of 0.32 km s^{-1} (on-line Hanning smoothed). The bandpass was centered at an LSR velocity of -55.0 km s^{-1}, and a rest frequency of 22,789.421 MHz was assumed for the transition. The flux density scale was set by assuming a flux density of 42 Jy for 3C 84.

The data were edited and calibrated at the VLA using standard DEC-10 reduction programs. Further data reduction procedures employed the AIPS (Astronomical Image Processing System) software package running on an Alliant VFX-40 computer. Images of the spectral line channels were made with a pixel size of 0".06 and 256 × 256 pixels. The resulting images have a resolution of 0".209 × 0".205 p.a. 80°. Channel zero of a VLA spectral line data base is a channel with a frequency bandwidth equal to 75% that of the total bandwidth. Since the signal to noise ratio of the channel zero map was significantly larger than that of other spectral channels containing maser features, an iterative self-calibration technique was applied to the channel zero data. The improved complex gains determined for channel zero were then applied to the other spectral channels. The ratio of signal to noise was sufficiently low (≈ 8) in the resulting spectral line images as to not require "cleaning" with a beam deconvolution algorithm. Since the line to continuum ratio was expected to be relatively small, a continuum image was subtracted from all of the channel maps. The continuum map was contracted from 79 spectral line channels free of emission. After the continuum subtraction step, the resulting channel images contained only unresolved point sources. Figure 1 shows a continuum image of NGC 7538 IRS 1. Two components are seen separated by 0".4 on a N-S line. The northern component is the double core source seen in the 2 cm data of Turner & Matthews (1984) and Campbell (1984). This component is not seen in our images as a double source because our angular resolution is slightly coarser than the separation between the two lobes. A comparison between the 2 cm data of Campbell (1984) or Turner & Matthews (1984) and the 1.3 cm data presented here is complicated not only by resolution differences but also by optical depth effects. Indeed, Campbell (1984) has shown that the northern of the two lobes of the double core has a larger optical depth at 2 cm.

[1] The National Radio Astronomy Observatory is operated by Associated Universities, Inc., under cooperative agreement with the National Science Foundation.

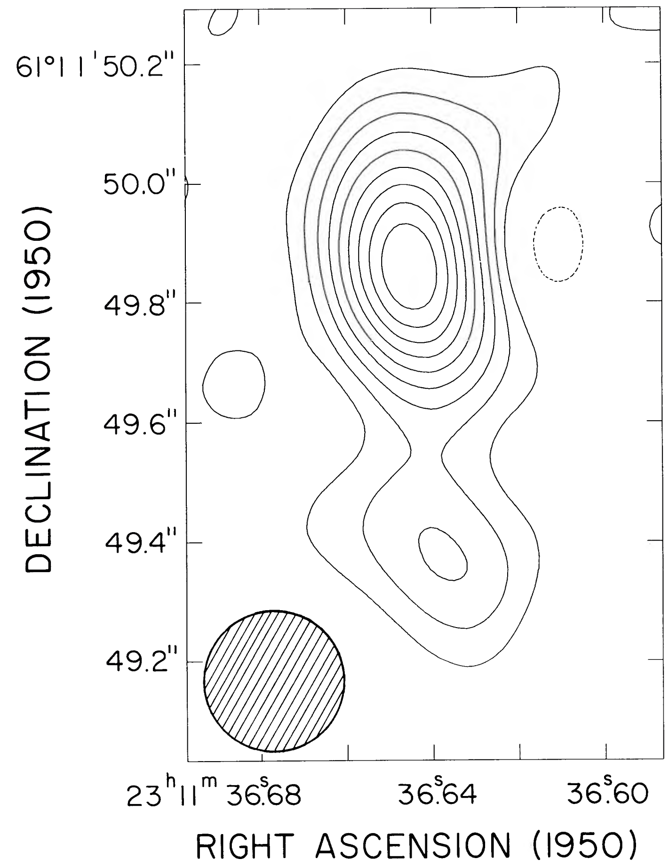

FIG. 1.—Radio continuum image of the IRS 1 region at 1.3 cm. The contours are at −10, 10, 20, 30, ..., 90% of the peak flux density of 89 mJy per 0".209 × 0".205 p.a. 80° beam.

Figure 2 is a spectrum of the line emission. It was obtained by summing the emission in the individual line channels within a box, 0".5 on a side, centered, on IRS 1. Summing the flux density over a significantly larger box does not give a reason-

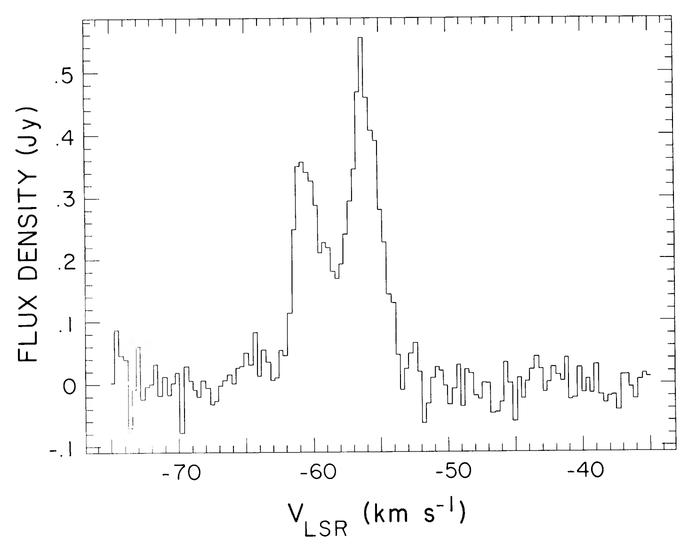

FIG. 2.—Spectrum of the $(J, K) = (3, 3)$ transition of $^{15}NH_3$ toward NGC 7538 IRS 1. The plot was made by summing emission in individual line channels within a box, 0".5 on a side, centered on the position of IRS 1. The line rest frequency assumed in the plot is 22,789.421 MHz.

TABLE 1

MASER DATA

VELOCITY (LSR) ($km\ s^{-1}$)	COORDINATES (1950) Right Ascension	Declination	FLUX DENSITY (Jy)
−52.8	$23^h11^m36\overset{s}{.}656$	$61°11'49\overset{''}{.}84$	0.11
−53.4	36.660	49.89	0.11
−53.7	36.656	49.90	0.09
−54.0	36.648	49.87	0.08
−54.4	36.649	49.90	0.16
−54.7	36.647	49.91	0.18
−55.0	36.646	49.90	0.24
−55.3	36.646	49.91	0.24
−55.6	36.642	49.91	0.29
−56.0	36.645	49.90	0.32
−56.3	36.644	49.90	0.34
−56.6	36.643	49.90	0.26
−56.9	36.643	49.87	0.17
−57.2	36.646	49.87	0.15
−57.6	36.651	49.80	0.15
−57.9	36.655	49.80	0.15
−58.2	36.654	49.80	0.18
−58.5	36.655	49.79	0.15
−58.9	36.657	49.80	0.12
−59.2	36.650	49.76	0.12
−59.5	36.641	49.69	0.16
−59.5	36.661	49.81	0.13
−59.8	36.642	49.70	0.16
−60.1	36.643	49.73	0.19
−60.5	36.639	49.71	0.24
−60.8	36.638	49.73	0.29
−61.1	36.634	49.71	0.27
−61.4	36.636	49.70	0.17
−61.7	36.631	49.76	0.14

able zero level for the spectrum due to an inadequate subtraction of the continuum emission. Within measurement errors the spectrum agrees quite well with the VLA and Bonn 100 m spectra presented by Johnston et al. (1989). Thus, there is no evidence for significant variability in the $^{15}NH_3$ integrated spectrum since 1983. This is suggestive evidence that the flux densities of individual $^{15}NH_3$ maser features are not highly time-variable.

The positions, velocities, and flux densities of the individual maser features are presented in Table 1. Positions of the masers were obtained by fitting a two-dimensional Gaussian profile to the image data. To preserve the accuracy of the absolute positions of the maser features reported in Table 1, the self-calibrated data were used to obtain only the relative positions between the individual maser features. The absolute positions of the maser features were obtained by referencing their relative positions to the fitted position of the maser feature at $-56.6\ km\ s^{-1}$ in a non–self-calibrated map. The absolute positional accuracy of the reference maser feature is estimated to be $0\overset{''}{.}1$. The positions of the individual maser features relative to the reference feature have an accuracy estimated at $0\overset{''}{.}02$. All of the Gaussian fits of the maser features are consistent with the maser features being unresolved in our $0\overset{''}{.}21$ beam. Assuming $0\overset{''}{.}15$ as an upper limit to the size of the maser features[2] implies a lower limit of 51,000 K for the brightness temperature of the maser with the largest flux density. This is a factor of ≈ 10 higher than the brightness temperature reported by Johnston et al. (1989) who found all of the maser features unresolved in a $1\overset{''}{.}2$ beam.

Figure 3*a* details the positions of the maser features with respect to the continuum image. The masers are found close to, but not necessarily coincident with the peak continuum emission. Figure 3*b* is a plot of the flux density of the maser features along with their positions relative to the continuum. The maser features are grouped according to flux density into six bins and their positions plotted with circle size proportional to the flux density of the individual features. The strongest masers are found in two groups, separated by approximately $0\overset{''}{.}2$ along a N-S line. Figure 3*c* is similar to Figure 3*b*, with circle size related to the LSR velocity of individual maser features. A trend in the velocities of the individual maser features is apparent in Figure 3*c*. The velocities of the maser features tend to increase in radial velocity with more NE position.

Detailed direct comparison of the positions and velocities of the individual $^{15}NH_3$ maser features mapped in this study to those of Johnston et al. (1989) is complicated by a number of factors, such as the different spectral and spatial resolutions employed. Despite these differences, there is agreement in the general distribution of the $^{15}NH_3$ masers reported here and by Johnston et al. (1989). In both studies, the $^{15}NH_3$ maser emission is found coincident with the peak NGC 7538 IRS 1 continuum emission. There is also agreement in the general distribution of individual maser features, and the present study confirms the velocity gradient in the $^{15}NH_3$ maser emission found by Johnston et al. (1989).

2.2. *Recombination Line Observations*

To aid in the determination of the kinematic relationship between the $^{15}NH_3$ molecular cloud and the NGC 7538 IRS 1 H II region, H 35α, H 42α, and H 76α recombination line data have been obtained. The H 35α line data were taken in 1989 August with the IRAM 30 m telescope. The telescope was pointed at the position of the IRS 1 H II region. The line rest frequency was taken as 147.046 GHz. At this frequency, the FWHP telescope beam is 15″. The receiver used was a superconducting mixed (SIS) receiver tuned for a single sideband response. The image response was 6 db below that of the signal. The system noise was 970 K, including corrections for the forward scattering efficiency (0.9) and beam efficiency (0.6), as well as radiation from the Earth's atmosphere and atmospheric absorption. The spectra were measured using position switching, with the reference 1 degree west of IRS 1. The frequency resolution used was 1 MHz (2.04 $km\ s^{-1}$ at the line rest frequency). The data were taken by integrating 30 s at the position of IRS 1, then 30 s on the reference. The spectra were produced from the average of pairs of such measurements; the total integration time was 68 minutes. The line intensity scale was determined by chopper wheel calibrations. Antenna temperature was converted to flux density by multiplying by 5.74. The rest frequency of the $J = 8$–7, $K = 6$ transition of CH_3CN is 9.914 MHz ($+20\ km\ s^{-1}$) from the rest frequency of the H 35α transition. The rest frequency of the $J = 8$–7, $K = 4$ line is within the instrumental bandpass, and was undetected, so that the weaker, $K = 6$, and higher K components will have no effect on the recombination line profile.

The calibrated H 35α spectrum is shown in Figure 4 (*histogram plot*). The line is asymmetric, with the main peak near $-70\ km\ s^{-1}$, and a wing near $-35\ km\ s^{-1}$. The smooth line in Figure 4 represents the sum of a two-component Gaussian fit of the data. The results of the fit are presented in Table 2.

[2] A typical maximum size of the maser spots calculated by a Gaussian fitting deconvolution algorithm is $0\overset{''}{.}15$.

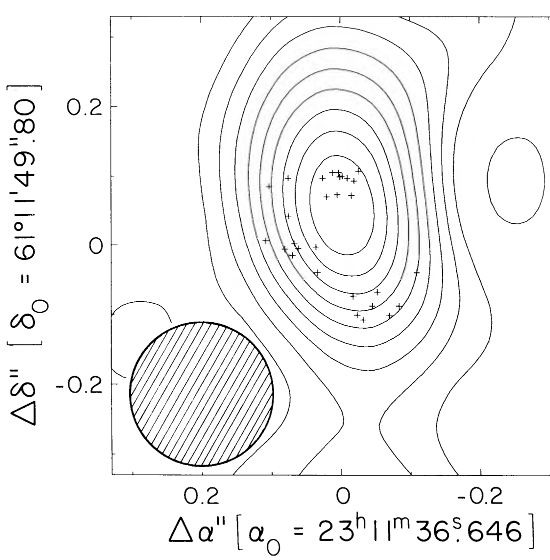

FIG. 3*a*

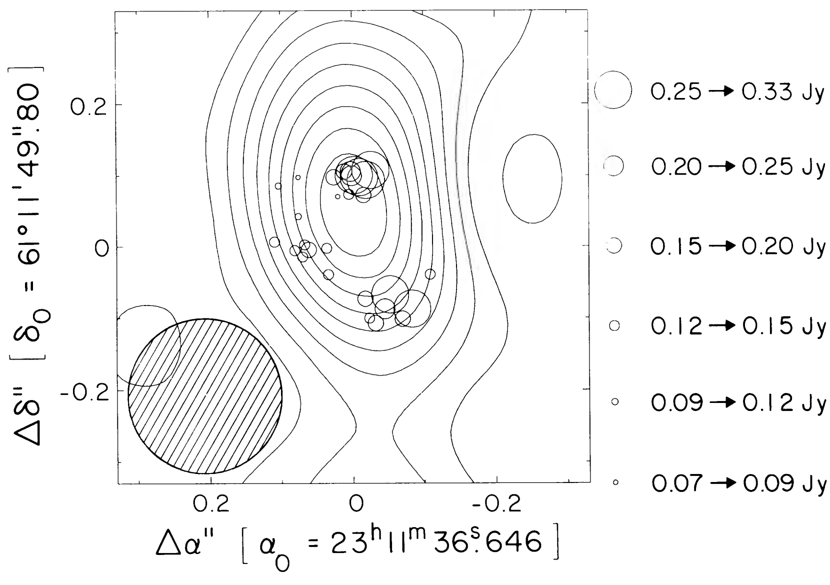

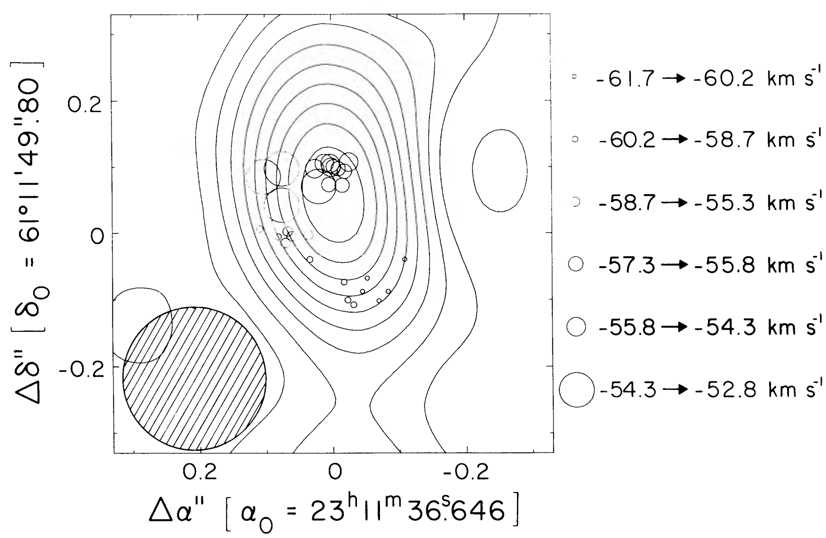

FIG. 3*c*

FIG. 3.—(*a*) Distribution of $^{15}NH_3$ maser emission toward the NGC 7538 IRS 1 region. The positions of individual maser features are indicated by crosses. The masers are superposed on 1.3 cm continuum emission (see Fig. 1). (*b*) Flux density distribution of the $^{15}NH_3$ masers associated with the NGC 7538 IRS 1 region. The circle size (*right side*) corresponds to different flux density ranges. The largest circle corresponds to the most intense emission range (0.25 to 0.33 Jy). The masers are superposed on contours of 1.3 cm continuum emission. (*c*) Velocity distribution of $^{15}NH_3$ masers associated with NGC 7538 IRS 1. The circle size (*right side*) corresponds to different velocity ranges. The largest circle corresponds to the most redshifted velocity bin (-54.3 to -52.8 km s^{-1}). The masers are superposed on contours of the 1.3 cm continuum emission.

The H 35α data suggest that there are two distinct recombination line velocity components contained within the 15″ beam. The stronger component has a velocity comparable to that of other spectral line observations of the NGC 7538 region. The weak component is redshifted with respect to the strong component by almost 40 km s^{-1}. The H 35α data, taken alone, do not allow a determination of the spatial location of the two components, other than that they are located within the FWHP beam, centered on the position of NGC 7538 IRS 1. Since the beam size (FWHP) is 15″, the source of the two components could be either the NGC 7538 IRS 1 or IRS 2 H II regions, which are separated by ≈8″ along a N-S line.

The H 42α data were taken with the Berkeley, Illinois, Maryland millimeter wave interferometer array, BIMA[3] over a 6 month period beginning in 1987 February. Thirteen baselines were used in mixed array configurations, with baseline lengths ranging from 13 to 58 m. The total integration time was approximately 8 hr. The FWHM of the resulting synthesized beam was 9″.5 × 9″.3 p.a. 101°. One hundred twenty-eight channels were used across a 40 MHz bandpass resulting in a channel separation of 1.09 km s^{-1} at the line rest frequency of 85.68842 GHz. The objects BL Lac and 3C 84 were used for phase, bandpass, and flux density calibration. The flux density of 3C 84 (28.3 Jy) was calibrated with respect to the planets

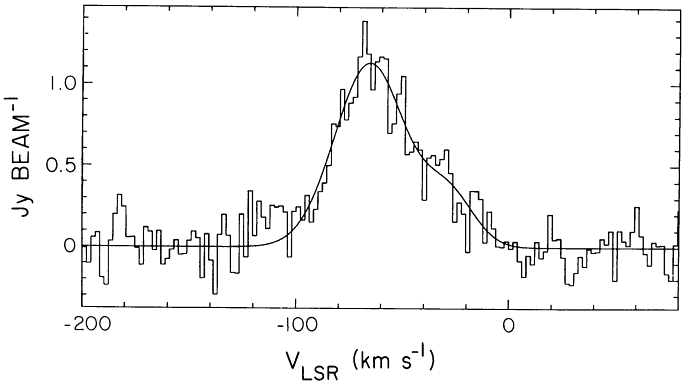

FIG. 4.—Histogram spectrum of the H 35α recombination line emission toward the NGC 7538 IRS 1 and IRS 2 regions observed with the IRAM 30 m telescope. Velocities are with respect to the local standard of rest, assuming a rest frequency of 147.046 GHz for the transition. The solid line represents the sum of a two-component Gaussian fit of the data.

Venus and Saturn, and remained constant throughout the observation period. The flux density of BL Lac steadily increased from 1.6 to 4.0 Jy throughout the duration of the observations. Twenty channels from each end of the resulting spectrum were averaged into a continuum image, which was then subtracted from the data. To increase sensitivity, the data were averaged over 10 km s^{-1} in the u, v plane, with the line images made at 5 km s^{-1} intervals.

The strongest line source in the H 42α data is centered at the position of the IRS 2 H II region. The single component Gaussian-fitted velocity of the spectral line at IRS 2 is -69 ± 4 km s^{-1}. A shift is seen in the peak velocity of the spectral line, moving south to the position of the IRS 1 H II region. The single-component Gaussian-fitted velocity of the line centered at the position of IRS 1 is -38 ± 4 km s^{-1}. Given the synthesized beam size of the observations, it is likely that the strong line from the IRS 2 H II region contaminates the Gaussian-fitted velocity of the weaker line found at IRS 1. Nevertheless, taken together, the H 42α and H 35α data allow an identification of the IRS 2 H II region at a velocity nearly that of the molecular cloud (≈ -65 km s^{-1}). Thus, the velocity of the IRS 1 H II region is redshifted with respect to the molecular cloud velocity by at least 20 km s^{-1} and perhaps up to 40 km s^{-1}.

The H 76α data were taken with the VLA on 1985 May 18. The VLA was in the B-array at the time, providing baselines ranging in length from 0.21 to 11.1 km. Twenty-three antennas and 32 spectral line channels were used in a 12.5 MHz bandwidth providing a channel separation of 7.97 km s^{-1} at the line rest frequency of 14.68999 GHz. On-line Hanning smoothing was used, and a bandpass correction was applied from observations of 3C 84. The bandpass was centered at a velocity of -62 km s^{-1}. The flux density scale was set from observations of 3C 286 (3.49 Jy). The phase calibrator was 2352+495. The data were edited and calibrated at the VLA using standard DEC-10 reduction programs. Further data reduction procedures employed the AIPS software package running on an Alliant VFX-40 computer. Maps of the spectral line channels were made with a pixel size of 0".1 and 512 × 512 pixels. A self-calibration algorithm was employed using channel 0 of the data set. A continuum image was made from six channels at the ends of the bandpass. The continuum image was subtracted from each individual channel to produce "line only" data cubes. To maximize the sensitivity to recombination line emission from the NGC 7538 IRS 1 H II region, the H 76α data were mapped with several u, v data Gaussian tapers. The tapers employed ranged from no taper at all, to a 30% taper at 100 kλ. Maps were made using both uniform and natural weighting of the u, v data in the Fourier transform gridding algorithm. The resulting images had spatial resolution ranging from 0".38 (uniform weighting, no taper) to 1".72 (natural weighting, 100 kλ taper).

[3] Operated by the University of California at Berkeley, the University of Illinois, and the University of Maryland, with support from the Natonal Science Foundation.

TABLE 2

RECOMBINATION LINE PARAMETERS

Region-Line	S_{pk} (mJy)	V_{lsr} (km s^{-1})	ΔV (km s^{-1})
Component 1 H 35α	300 ± 50	-28.6 ± 4.1	28.5 ± 6.6
Component 2	1100 ± 10	-65.6 ± 1.4	38.6 ± 3.9
IRS 1 H 42α	260 ± 130	-38 ± 4	46 ± 10
IRS 2	400 ± 130	-69 ± 4	47 ± 5
IRS 1 H 76α	8 ± 0.5	-21.5 ± 1.7	47.1 ± 3.0
IRS 2	293 ± 7	-65.4 ± 0.03	24.6 ± 0.1

Line emission toward the IRS 1 and 2 regions was evident using all combinations of weighting and tapering. However the signal-to-noise ratio was most optimum for the IRS 1 and IRS 2 images using a combination of natural weighting and no taper with a resulting resolution of 0".62 × 0".53 p.a. 73° (IRS 2) and natural weighting with a 400 kλ taper with a resolution of 0".76 × 0".66 p.a. 88° (IRS 1). Flux density within an irregular area covering a spatial extent of the continuum emission was summed for the IRS 1 and IRS 2 regions in all spectral channels. The extent of the area in the summation was 4.4 and 105 arcsec^2 for the IRS 1 and IRS 2 spectra, respectively. These summed fluxes were used to produce the H 76α spectra for the IRS 2 and IRS 1 regions (*histogram plots*) shown in Figure 5. Also shown in this figure are single-component Gaussian fits of the spectra (*smooth lines*). Parameters of the fits are presented in Table 2. The fitted velocity of the IRS 2 H 76α line, shown in Figure 5 (*top panel*), agrees quite well with the fitted velocity of the H 42α line, and the strong H 35α component. The Gaussian fitted velocity of the H 35α weaker component is blueshifted 7 km s^{-1} with respect to the IRS 1 H 76α line. The Gaussian fit of the velocity of the IRS 1 H 42α component is blueshifted 16 km s^{-1} with respect to the fitted velocity of the H 76α line; however, as discussed previously, the H 42α line toward IRS 1 is likely contaminated by the stronger IRS 2 line, possibly resulting in a more blueshifted velocity.

3. DISCUSSION

From the plots of radial velocities and flux densities of the ammonia maser velocity components, it seems likely that the apparent distribution of the ammonia masers is partially due to the orientation of the two bright background continuum sources being amplified by a foreground molecular cloud. Figure 3*b* shows that the brightest masers are found in two groups separated by approximately 0".2. The orientation and positions of the two maser groups is similar to that of the double-lobe continuum emission core reported by Turner & Matthews (1984) and Campbell (1984). Unfortunately, the

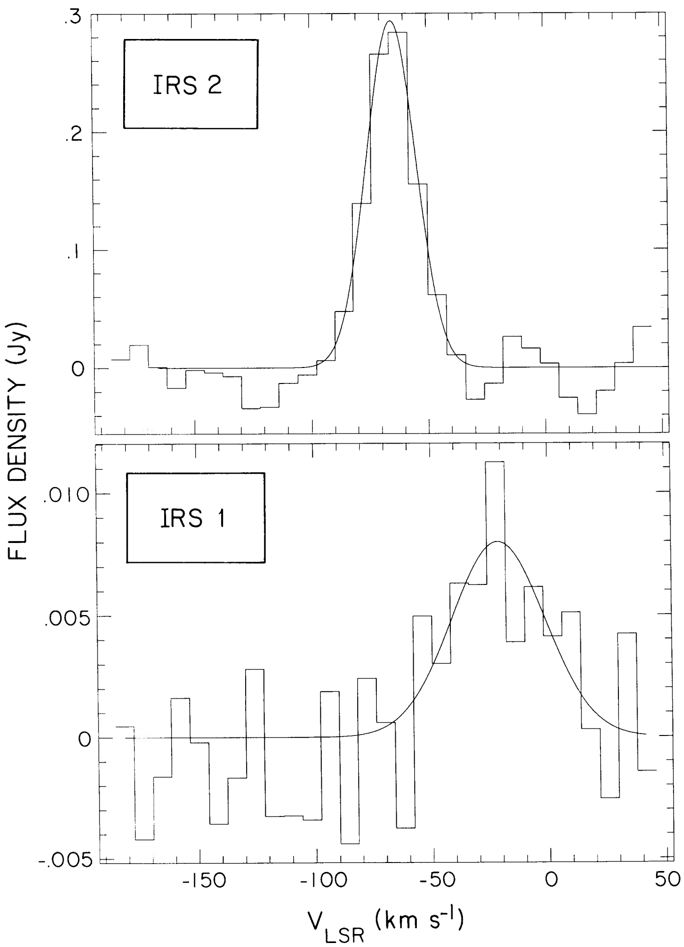

FIG. 5.—Histogram spectrum of the H 76α recombination line emission toward the IRS 2 region observed with the VLA interferometer with a resolution of 0".62 × 0".53 p.a. 73° (*top panel*). Velocity is with respect to the local standard of rest, assuming a rest frequency of 14.68999 GHz for the transition. The solid line represents a Gaussian fit of the data. The bottom panel shows a histogram spectrum of the H 76α recombination line emission toward the IRS 1 region with a resolution of 0".76 × 0".66 p.a. 88°. The solid line represents a Gaussian fit of the data.

Campbell (1984) and Turner & Matthews (1984) observations disagree on the absolute position of the double-lobe core by $\Delta\alpha = 0\farcs3$, $\Delta\delta = 0\farcs1$, and the current observations do not have sufficient spatial resolution to resolve the continuum source. Therefore, confirmation that the strongest $^{15}NH_3$ masers are indeed amplifying continuum photons from the double-lobe core must await higher resolution $^{15}NH_3$ spectral line and continuum observations.

Given the peak temperature of the brightest maser (calculated in § 2) and assuming a continuum brightness temperature of 10^4 K, a calculation of the maser optical depths is possible. With a minimum excitation temperature (compared to the background continuum temperature) for a completely unsaturated maser the optical depth is -1.6. For a completely saturated maser the optical depth is -5.1. In either case, the optical depth is appreciable. In the lower resolution maps of Johnston et al. (1989), the maximum line optical depth was estimated to be -0.5.

The column density of $^{14}NH_3$ in absorption for this source is 2.5×10^{18} cm^{-2} (Wilson et al. 1983). This is a total column density assuming that all levels are thermalized with a rotational temperature of 220 K. Taking the isotope ratio, $^{14}NH_3/^{15}NH_3$, to be 300, we find that the total column density in the $^{15}NH_3$ species is 10^{16} cm^{-2}. Since the optical depths in the rarer species are lower, the population of nonmetastable levels probably have only 10% of the population of metastable levels. Using the formulae quoted by Pauls et al. (1983), we predict a column density in the $(J, K) = (3, 3)$ levels of 3×10^{15} cm^{-2} for a rotational temperature of 150 K. Applying the relation between column density and optical depth to the integrated line profile gives a value of 22 for the absolute value of the product of peak optical depth and excitation temperature, T_x. From the model calculation for the excitation of the $^{15}NH_3$ $(J, K) = (3, 3)$ masers in Mauersberger et al. (1986), we find $|T_x| = 11.5$ K. Then the peak optical depth would be -1.9, which is about half that found for the maximum optical depth under the assumption of complete maser saturation. This analysis makes the strong prediction that these masers will be resolved by future observations employing a beam size of $< 0\farcs13$.

As seen in Figure 3*c*, the radial velocities of the maser features generally increase to the NE. If this velocity gradient is balanced by gravity then the total mass interior to the rotating molecular material is about 10 $M_\odot$. The orientation of the velocity shift appears to have a significant E-W component. Scoville et al. (1986) made 7" resolution maps of the ^{13}CO emission toward NGC 7538. Their data show a rotating ^{13}CO structure centered on the position of IRS 1. The ^{13}CO emission is elongated E-W, having an extent of approximately 20". Their data show a velocity shift of about 8 km s^{-1} from the east to west edge. The recent ^{13}CO data of Pratap et al. (1991) taken with the BIMA millimeter array, although showing a considerably more complicated ^{13}CO distribution than the Scoville et al. (1986) data, confirms the existence of a rotational component in the ^{13}CO emission near IRS 1. The data in Figure 2 of Pratap et al. (1991) show both a greater velocity extent in the east-west gradient (≈ 10 km s^{-1}), and a greater spatial extent (≈ 60"). Compared to the maps of Scoville et al. (1986), some of the additional complexity of the Pratap et al. (1991) ^{13}CO map can be attributed to a combination of greater instrumental sensitivity and inclusion of short *u*, *v* spacing information. The Pratap et al. (1991) data may also be complicated by the detection, in ^{13}CO, of another source of CO emission ≈ 15" south of IRS 1 (see Pratap, Batrla, & Snyder 1990). The orientation of the ^{13}CO velocity gradient for both the Scoville et al. (1986) and Pratap et al. (1991) data is the same as that evident in the $^{15}NH_3$ maser data: redshifted velocities to the east, and blueshifted velocities to the west. This suggests that the ^{13}CO emission and the $^{15}NH_3$ masers are both tracing the kinematics of a rotating molecular cloud surrounding the IRS 1 region. The ^{13}CO IRS 1 molecular cloud probably plays a significant role in the evolution of the IRS 1 H II region.

The radio continuum and recombination line data allow an estimate of the electron temperature, T_e, of the ionized gas. Assuming LTE conditions, small continuum and line opacities, and that the fractional abundances of ionized helium is equal to 10%, we calculate $T_e = 22{,}000$ K using equation (1) of Pauls & Wilson (1977). As noted by Schilke et al. (1990, Fig. 3) the continuum emission from NGC 7538 IRS 1 is very complex, and thus the value of T_e is rather uncertain. More definite is the kinematic relationship between the IRS 1 H II region and the $^{15}NH_3$ masers (and indeed the entire molecular cloud). This is also of great interest. The average velocity of the $^{15}NH_3$

masers is -57.3 km s^{-1}, with a spread in the velocities of ± 4.5 km s^{-1}. Indeed, the velocity of the $^{15}NH_3$ masers is similar to that of all other molecular cloud velocity tracers observed in the NGC 7538 region. The recombination line velocity of the IRS 2 region is also quite similar (-65 km s^{-1}) to that of the molecular cloud. However, the H 76α, H 42α, and H 35α recombination line data, taken together, indicate that the IRS 1 H II region is redshifted by between 20 and 40 km s^{-1} with respect to the molecular cloud material.

The redshifted velocity of the IRS 1 H II region is particularly difficult to understand in light of the current and previously published molecular observations of the IRS 1 region. Because of their similar LSR velocities, we assume the plethora of intense maser emission lines toward IRS 1 arise from molecules in the NGC 7538 molecular cloud. This assumption then localizes the IRS 1 H II complex to the NGC 7538 molecular complex, since strong maser emission is generally closely associated with H II regions. This conclusion is also suggested by the ^{13}CO observations, which show a rotating structure at the velocity of the molecular cloud surrounding the IRS 1 H II region. Available evidence then suggest that the IRS 1 region is an integral part of the NGC 7538 complex. We suggest that the central star(s) of IRS 1 formed toward the back face of the NGC 7538 molecular cloud and is nearly at rest with respect to the cloud. The velocity of the center of mass of the IRS 1 system is represented by the average velocity of the rotating ^{13}CO structure. The masers then have a velocity within a few km s^{-1} of the center of mass of the system, as is the case for other well studied regions of star formation. The between 20 and 40 km s^{-1} redshifted recombination line velocity of IRS 1 is rather large, but may be explained as a champagne flow directed away from the Earth (e.g., Tenorio-Tagle, Yorke, & Bodenheimer 1979) created as the ionization front of the IRS 1 H II region broke through the edge of the ambient molecular cloud. This allowed the high pressure and temperature ionized hydrogen within the H II region to be channeled into the lower density and pressure intercloud medium. Computer modeling of champagne flows (Tenorio-Tagle et al. 1979, and references therein) indicate ionized hydrogen velocities in low-density gas ($\approx 10^2$ to 10^3 cm^{-3}), similar to the redshifted velocity of the NGC 7538 IRS 1 H II region. Current champagne flow models do not include the effects of massive stellar wind outflows from the exciting central stars. It is possible that in regions like NGC 7538 IRS 1 a strong stellar wind also plays a significant role in accelerating the ionized hydrogen to the observed redshifted velocity.

It appears unlikely that NGC 7538 IRS 1 is powered by a "runaway" OB star moving through the interstellar medium (see e.g., Van Buren et al. 1990 for a summary of such models). In this collision model, the runaway OB star is moving into the NGC 7538 molecular cloud with a projected velocity of ≈ 40 km s^{-1}. Since the recombination line data show the velocity of the IRS 1 region redshifted with respect to that of the molecular cloud, the leading edge of the H II region, where strong masers are thought to occur in this model, will be located on the opposite side of the H II region from the Earth. Since the IRS 1 H II region is optically thick at 18 cm (the wavelength of the OH maser transition) the OH maser emission would be greatly attenuated by the H II region; strong OH maser emission would not be observed. In addition, if the collision scenario were correct, it would be difficult to explain the rotating ^{13}CO structure centered on IRS 1. Therefore, this scenario appears unlikely.

4. CONCLUSIONS

The $^{15}NH_3$ $(J, K) = (3, 3)$ maser emission toward NGC 7538 IRS 1 has been imaged with 0".2 resolution. The masers are distributed in a region slightly larger than 0".2 near the core of the H II region associated with IRS 1. The strongest masers are distributed in two groups separated by approximately 0".2 on a north-south line. These masers are probably amplifying the strong background continuum of the double-lobe radio continuum core of the H II region associated with NGC 7538 IRS 1. The velocities of the $^{15}NH_3$ masers show a gradient to the NE. The orientation of the gradient is the same as that found by Scoville et al. (1986) for the ^{13}CO emission toward IRS 1. Both the ^{13}CO emission and the $^{15}NH_3$ masers probably arise in a thick rotating molecular disk surrounding IRS 1, which probably has a significant effect on the evolution of the IRS 1 region.

Hydrogen recombination line observations at the H 35α, H 42α, and H 76α transitions are presented. These data show that the ionized hydrogen in the NGC 7538 IRS 1 H II region is significantly redshifted with respect to the LSR velocity of the NGC 7538 molecular cloud. The redshift may be as much as 40 km s^{-1}. The LSR velocity of the IRS 2 H II region is similar to that of the molecular cloud. Models suggesting that IRS 1 is a foreground or background object, or that IRS 1 is an object colliding and passing through the NGC 7538 molecular cloud are unlikely. The observed redshifted velocity of the IRS 1 H II region may be explained as an ionized hydrogen champagne flow directed away from the Earth. A strong stellar wind outflow from the IRS 1 central stellar source may also play a role in producing the observed velocity of the IRS 1 H II region.

REFERENCES

Campbell, B. 1984, ApJ, 282, L27

Dickel, H. R., Rots, A. H., Goss, W. M., & Forster, J. R. 1982, MNRAS, 198, 265

Fischer, J., Righini-Cohen, G., Simon, M., Joyce, R. R., & Simon, T. 1980, ApJ, 240, L95

Johnston, K. J., Stolovy, S. R., Wilson, T. L., Henkel, C., & Mauersberger, R. 1989, ApJ, 343, L41

Kameya, O., Morita, K., Kawabe, R., & Ishiguro, M. 1990, ApJ, 355, 562

Lada, C. J. 1985, ARA&A, 23, 267

Madden, S. C., Irvine, W. M., Matthews, H. E., Brown, R. D., & Godfrey, P. D. 1986, ApJ, 300, L79

Martin, A. H. 1973, MNRAS, 163, 141

Mauersberger, R., Wilson, T. L., & Henkel, C. 1986, A&A, 160, L13

Menten, K. M., Walmsley, C. M., Henkel, C., & Wilson, T. L. 1986, A&A, 157, 318

Pauls, T. A., & Wilson, T. L. 1977, A&A, 60, L31

Pauls, T. A., Wilson, T. L., Bieging, J. H., & Martin, R. N. 1983, A&A, 124, 23

Pratap, P., Batrla, W., & Snyder, L. E. 1989, ApJ, 341, 832

———. 1990, ApJ, 351, 530

Pratap, P., Snyder, L. E., & Batrla, W. 1991, in Proceedings of the Third Haystack Conference on Atoms, Ions, and Molecules, ed. A. D. Haschick & P. T. P. Ho (ASP Conf. Ser.), in press

Reid, M. J., & Moran, J. M. 1981, ARA&A, 19, 231

Rots, A. H., Dickel, H. R., Forster, J. R., & Goss, W. M. 1981, ApJ, 245, L15

Schilke, P., Mauersberger, R., Walmsley, C. M., & Wilson, T. L. 1990, A&A, 227, 220

Scoville, N. Z., Sargent, A. I., Sanders, D. B., Claussen, M. J., Masson, C. R., Lo, K. Y., & Phillips, T. G. 1986, ApJ, 303, 416

Tenorio-Tagle, G., Yorke, H. W., & Bodenheimer, P. 1979, A&A, 80, 110

Turner, B. E., & Matthews, G. E. 1984, ApJ, 277, 164

Van Buren, D., Mac Low, M. M., Wood, D. O. S., & Churchwell, E. 1990, ApJ, 353, 570

Wilson, T. L., Mauersberger, R., Walmsley, C. M., & Batrla, W. 1983, A&A, 127, L19